PAPER

Field induced spin freezing and low temperature heat capacity of disordered pyrochlore oxide $Ho_2Zr_2O_7$

To cite this article: Sheetal *et al* 2022 *J. Phys.: Condens. Matter* **34** 245801

IOP Publishing Journal of Physics: Condensed Matter
J. Phys.: Condens. Matter **34** (2022) 245801 (7pp) https://doi.org/10.1088/1361-648X/ac5fd8

Field induced spin freezing and low temperature heat capacity of disordered pyrochlore oxide $Ho_2Zr_2O_7$

Sheetal[1], A Elghandour[2], R Klingeler[2] and C S Yadav[1,*]

[1] School of Basic Sciences, Indian Institute of Technology Mandi, Mandi-175075 (H.P.), India
[2] Kirchhoff Institute of Physics, Heidelberg University, INF 227, D-69120 Heidelberg, Germany

E-mail: shekhar@iitmandi.ac.in

Received 3 February 2022, revised 12 March 2022
Accepted for publication 22 March 2022
Published 7 April 2022

Abstract

Spin ice materials are the model systems that have a zero-point entropy as $T \to 0$ K, owing to the frozen disordered states. Here, we chemically alter the well-known spin ice $Ho_2Ti_2O_7$ by replacing Ti sites with isovalent but larger Zr ion. Unlike the $Ho_2Ti_2O_7$ which is a pyrochlore material, $Ho_2Zr_2O_7$ crystallizes in disordered pyrochlore structure. We have performed detailed structural, ac magnetic susceptibility and heat capacity studies on $Ho_2Zr_2O_7$ to investigate the interplay of structural disorder and frustrated interactions. The zero-field ground state exhibits large magnetic susceptibility and remains dynamic down to 300 mK without showing Pauling's residual entropy. The dynamic state is suppressed continuously with the magnetic field and freezing transition evolves ($\sim$10 K) at a field of $\sim$10 kOe. These results suggest that the alteration of chemical order and local strain in $Ho_2Ti_2O_7$ prevents the development of spin ice state and provides a new material to study the geometrical frustration based on the structure.

Keywords: frustrated magnetism, pyrochlores, spin freezing

(Some figures may appear in colour only in the online journal)

1. Introduction

Beginning with the identification of unusual disordered ground state in magnetic materials, frustration becomes a source of fascination among the scientists. In these systems, pyrochlore $A_2Ti_2O_7$ (A = Dy, Ho) as an exemplar of three-dimensional frustration continues to be the central topic of research due to the observation of water ice-like highly degenerate macroscopic ground state [1, 2]. $Dy_2Ti_2O_7$ and $Ho_2Ti_2O_7$ are the well-known spin ice materials that possess the finite residual entropy at the lowest temperature which is equivalent to the Pauling's value of water ice [2, 3]. Apart from the spin-ice behavior below $\sim$2 K, $Dy_2Ti_2O_7$ also shows a strong frequency-dependent spin-freezing at $\sim$16 K [4, 5]. However no such feature is seen for the $Ho_2Ti_2O_7$ which distinguishes the spin dynamics of $(Ho/Dy)_2Ti_2O_7$ [6, 7].

In order to understand the spin-ice state, researchers have begun to look outside the present structural map scenario by forming the stuffed pyrochlores by placing a non-magnetic atom or the atoms with smaller moments in the pyrochlore lattice [8–14]. In pyrochlore oxide $A_2B_2O_7$, various combinations of A and B site ions are employed to replace the existing spin ice state and disorder the symmetry of available crystal structure. The zirconate and hafnates pyrochlore provides a new avenue to look for a similar magnetic ground state. The stability of the pyrochlore structure can be empirically investigated in terms of atomic radii ratio (r_A/r_B) of the respective A and B ions [15]. The stable pyrochlore structure can be realized only for the range of $1.48 \leqslant r_A/r_B \leqslant 1.71$ ratio, and any deviation from this value disturbs the structural symmetry [15, 16]. For comparison, the radius ratio for $Dy_2Zr_2O_7$ and $Ho_2Zr_2O_7$ lies between 1.39 and 1.44, which is smaller than the nominal range for pyrochlore structure. These materials exhibit disordered pyrochlore structures and show the

* Author to whom any correspondence should be addressed.

absence of low-temperature magnetism of rare-earth moments. For example, $Pr_2Zr_2O_7$ exhibits spin ice-like correlations and strong quantum fluctuations [8, 9]. $Nd_2Zr_2O_7$ reveals the coexistence of an ordered and fluctuating Coulomb phase at low-temperature [10]. $Dy_2Zr_2O_7$, $Tb_2Hf_2O_7$ and $Pr_2Hf_2O_7$ remain dynamic down to 100 mK [11–13]. However the $Dy_2Zr_2O_7$ and $Pr_2Hf_2O_7$ have been shown to exhibit glassy transition at ∼90 mK [11, 17]. $Nd_2Hf_2O_7$ shows a long-range antiferromagnetic state ($T_N \sim 0.55$ K) with an all-in-all-out (AIAO) spin configuration [18]. Recent research also shows the loss of spin ice ground state due to a large chemical disorder induced by the stuffing of pyrochlores [11, 19].

There are few reports on the evolution of structure and magnetism of the magnetically diluted pyrochlore lattice under the application of magnetic field [16, 20, 21]. It was found that the structural disorder and spin ice state can be stabilized in disordered pyrochlores either by the application of magnetic field or by suitable choice of non-magnetic substitution over A site [16, 19]. $Dy_2Zr_2O_7$ shows the stabilization of spin-ice entropy in the presence of the magnetic field, and $Nd_2Zr_2O_7$ shows a field-induced one-dimensional quantum chain in AIAO [19, 20]. The substitution of non-magnetic La^{3+} ion in $Dy_2Zr_2O_7$ induces the structural change from disordered pyrochlore to a stable pyrochlore structure and observation of spin freezing at $H = 0$ Oe similar to the field-induced spin freezing of $Dy_2Zr_2O_7/Ho_2Ti_2O_7$ and the well-known spin ice system $Dy_2Ti_2O_7$ [16, 22]. In our previous work, we have reported the complete magnetic and structural phase diagram of $Dy_2Zr_2O_7$ and the evolution of pyrochlore phase and spin freezing transition on diluting $Dy_2Zr_2O_7$ by non-magnetic La over Dy. Further, pressure effects exhibit weak pyrochlore-type ordering in case of $Ho_2Zr_2O_7$ and $Er_2Zr_2O_7$ [21].

In this paper, we have studied a less explored disordered pyrochlores zirconate $Ho_2Zr_2O_7$ and discussed its structural, magnetic, and thermodynamic properties. We observe that with the stuffing of Zr on the Ti site, the spin ice character is completely lost. The large susceptibility and heat capacity values reveal a very dynamic ground state down to 300 mK. However, we found evidence of field-induced spin freezing at ∼10 K similar to the spin ice $Ho_2Ti_2O_7$ [7]. This also rules out the importance of high-temperature spin freezing in the formation of spin ice state below 1 K in $Dy_2Ti_2O_7$ [4].

2. Experimental details

The polycrystalline $Ho_2Zr_2O_7$ and $La_2Zr_2O_7$ compounds were prepared by solid-state reaction method using stoichiometric amounts of Ho_2O_3 (⩾99.99% purity), La_2O_3 (⩾99.999% purity) and ZrO_2 (99% purity). The raw oxides were pre-heated at 500 °C at weighed at 100 °C to avoid moisture because of their hygroscopic nature. The stoichiometric mixture of constituent oxides is heated twice at 1350 °C for 50 h with intermediate grindings, and the final heat treatment was given in the pellet form at the same temperature [19]. X-ray diffraction (xrd) experiment was performed using Rigaku x-ray diffractometer with Cu K_α source of wavelength 1.5406 Å in the 2θ range of 10–90°. The crystal structure and phase purity were confirmed by performing Rietveld refinement of the powder sample using Fullprof Suit software and the graphical interface Vesta [23]. The magnetic measurements were carried out using Quantum Design built magnetic property measurement system. Heat capacity measurements were measured using Quantum Design built physical property measurement system (PPMS) down to 1.8 K. Low temperature (300 mK to 4 K) specific heat measurements were performed using the dilution refrigerator option of PPMS using a relaxation method on a pressed pellet of ∼11.32 mg.

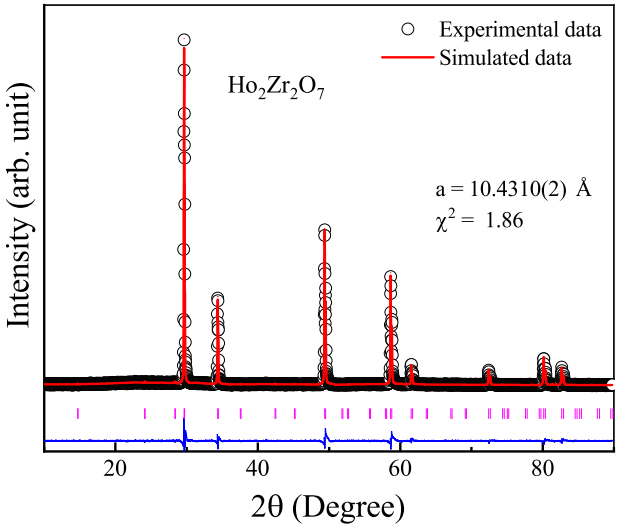

Figure 1. Room temperature x-ray powder diffraction pattern along with the Rietveld refined simulated data for $Ho_2Zr_2O_7$. As seen from the figure, the superstructure peaks corresponding to pyrochlore phase are missing.

Table 1. Positional parameters of $Ho_2Zr_2O_7$.

Atom	Wyckoff position	Fractional coordinates
Ho	16d	0.5, 0.5, 0.5
Zr	16c	0, 0, 0
O	48f	0.3726(17), 0.125, 0.125
O′	8b	0.375, 0.375, 0.375

3. Results and discussion

X-ray powder diffraction characterized the $Ho_2Zr_2O_7$ in single phase without any detectable impurity (see figure 1). Modeling of the xrd data with the cubic space group is consistent with the disordered pyrochlore structure and gives an excellent fit with $Fd\bar{3}m$ space group. The obtained crystallographic parameters are listed in table 1. Similar to the $Dy_2Zr_2O_7$ the xrd pattern of $Ho_2Zr_2O_7$ consists of only the main peaks of pyrochlore structure and the remaining superstructure peaks expected at $2\theta = 14°, 27°, 36°, 42°$ etc are missing [19, 24]. This behavior is consistent with the r_A/r_B ratio (∼1.40) of the compound, which is less than the value at which a stable pyrochlore structure is expected to evolve ($1.48 \leqslant r_A/r_B \leqslant 1.72$). Figure 2 shows the crystal structure of stable pyrochlore (a), disordered pyrochlore (b) and a comparison of fluorite and pyrochlore structure (c).

Unlike the configuration of oxygen atoms in the pyrochlore structure, the oxygen atoms locally form a perfect cube around

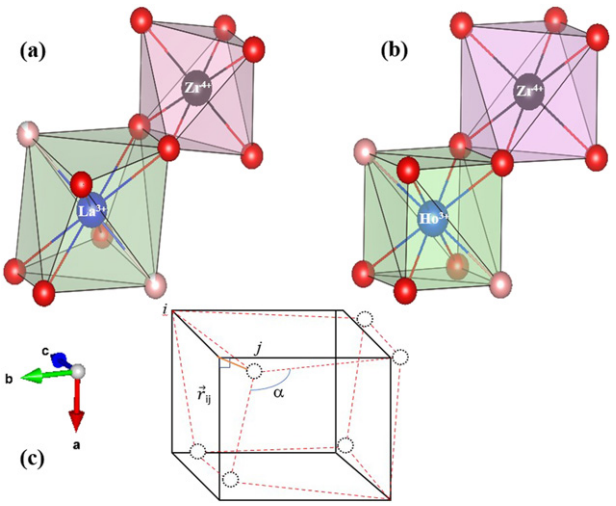

Figure 2. Coordination of A^{3+} and B^{4+} ions in $A_2B_2O_7$. (a) Pyrochlore structure: O^{2-} ions around A^{3+} (blue) rare-earth ion and B^{4+} (black) transition-metal ion form the distorted cube and octahedra respectively. The two types of oxygen are shown in red and light red color. (a) Pyrochlore (b) disordered pyrochlore structure of $Ho_2Zr_2O_7$. (c) Shows the difference between cubes of the fluorite and pyrochlore structures. For fluorite $\alpha = 90^\circ$ (angle between O–A–O) and all the oxygens are equivalent to the central ion. The $\vec{r}_{ij}$ is the unit vector showing displacement of O^{2-} ion from the ideal position. The deviation from fluorite structure can be parameterized in term of $\vec{r}_{ij}$.

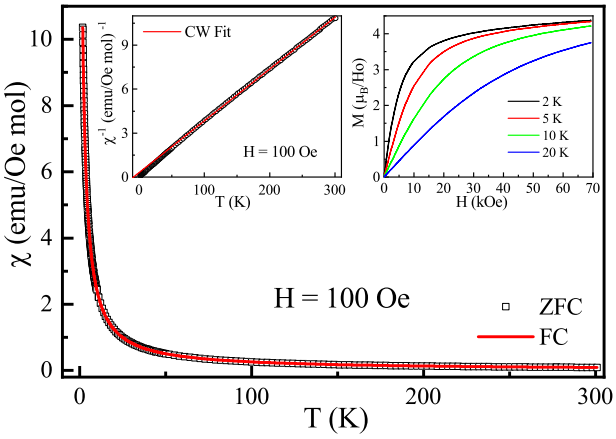

Figure 3. Temperature dependence of dc susceptibility in the range $T = 1.8$–300 K. The left inset shows Curie–Weiss fit to the inverse susceptibility data above 300 K. The right inset depicts isothermal magnetization as a function of the applied field showing a saturation moment of ∼4 μ_B/Ho ion at 2 K in addition to a finite slope indicating admixture of higher crystal field (CF) levels.

both the A and B sites in fluorite structure. The structural change from fluorite to pyrochlore phase, which consists of ordered oxygen vacancies, results in the shift in x-coordinate of 48f oxygen site. The variation in α and $\vec{r}_{ij}$ values can be used as a distortion parameter to study the difference between these structures. Depending on the choice of A and B atoms, the crystal symmetry changes and modifies the distortion parameters. It is worth mentioning that the pyrochlore compound $La_2Zr_2O_7$ with $\alpha = 108.65(19)$ and $|\vec{r}_{ij}| > 0$, shows a change of 12.96% from fluorite structure ($\alpha = 90$ and $|\vec{r}_{ij}| = 0$). In $Ho_2Zr_2O_7$, the obtained $\alpha = 91.085(10)$ and percentage deviation are 0.934%, indicating a small deformation from the fluorite structure.

Fitting of the inverse susceptibility data collected at 100 Oe above 80 K (left inset of figure 3) by Curie–Weiss law yields an antiferromagnetic Curie–Weiss temperature $\theta_{CW} \sim -10.7$ (4) K and effective magnetic moment $\mu_{eff} \sim 7.6$ (05) μ_B/Ho. Though the spin ice pyrochlore systems show crystal field anisotropy, phenomenologicaly the low-temperature (below $T = 30$ K) behavior can again be described by a Curie–Weiss law with the parameters viz $\theta_{CW} \sim -0.5$ K and $\mu_{eff} \sim 7.2$ μ_B/Ho. These parameters are similar to that for $Dy_2Zr_2O_7$. Here, it is worthy to mention that a ferromagnetic $\theta_{CW} \sim +1.9$ K was reported for the clean pyrochlore $Ho_2Ti_2O_7$ system [25]. The isothermal magnetization as a function of applied field for $Ho_2Zr_2O_7$ at various temperatures is shown in the right inset of figure 3. The saturation magnetization (M_s) at the maximum field (70 kOe) is comparatively less compared to the $Ho_2Ti_2O_7$ ($M_s \sim 5$ μ_B/Ho), which is half of the free-ion value and is due to the presence of strong crystal field anisotropy. These data indicate that $Ho_2Zr_2O_7$ exhibits strong anisotropic behavior like other systems such as $Ho_2Ti_2O_7$, $Dy_2Ti_2O_7$ and $Dy_2Zr_2O_7$ [19, 25, 26].

Figure 4 shows the ac susceptibility data for $Ho_2Zr_2O_7$ collected between the temperature range 1.8–40 K, at $H_{ac} = 2$ Oe, $f = 931$ Hz and in various dc magnetic fields ($H = 0$–30 kOe). Measurement of the real part of ac susceptibility in the absence of dc magnetic field shows paramagnetic-like behavior down to 1.8 K (figure 4(a)), similar to the behavior of spin ice $Ho_2Ti_2O_7$, which exhibits spin freezing anomaly at ∼16 K in the presence of magnetic field [3]. The large susceptibility value suggests the large spin dynamics down to the lowest measuring temperature. No anomaly appears up to 8 kOe except that of reduction in the magnitude of susceptibility, which indicates slowing down the spin dynamics with the field. A broad hump-like feature shows up at $H = 10$ kOe (around 10 K), and it shifts to higher temperatures with increasing the applied magnetic field. It is worthy of mentioning that $Dy_2Zr_2O_7$ shows the freezing anomaly in the presence of dc field of 5 kOe. Here, this feature is not seen even up to the field of 8 kOe, which is consistent with the large structural disorder in $Ho_2Zr_2O_7$ compared to $Dy_2Zr_2O_7$. It suggests that $Ho_2Zr_2O_7$ requires the higher field to slow down the spin dynamics induced by the large chemical disorder with Zr substitution at the Ti site. It is to note that the structurally ordered $Ho_2Ti_2O_7$ system shows the thermally activated high-temperature spin freezing behavior in the presence of a magnetic field, which rules out the importance of these features in the formation of spin ice state at low-temperature [27]. Inset of figure 4(a) shows the ac susceptibility data collected at various frequencies between 10 Hz–1 kHz in a field of 10 kOe. The frequency dependence of freezing anomaly is characterized by calculating the Mydosh parameter ($p = \delta T/T_f \ln f$), which comes out to be 0.18. This large value rules out the spin-glass behavior for which p values range between 0.005 to 0.01 and show the unusual spin freezing in these systems [28].

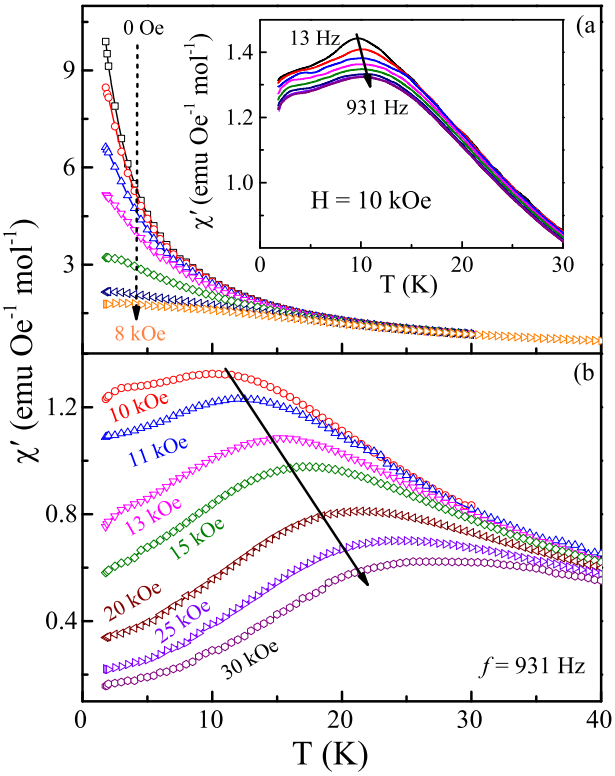

Figure 4. Real part of ac susceptibility data at 931 Hz in the presence of dc magnetic field ($H \leqslant 30$ kOe). Inset shows the frequency dependence of χ' at 10 kOe at various frequencies ranges between 10 Hz to 1 kHz.

The specific heat of $Ho_2Zr_2O_7$ down to 300 mK (shown in figure 5(a)) does not show any evidence of phase transition. Instead, the low-temperature heat capacity of the Ho based pyrochlore system shows an increase below $T = 1$ K, which is attributed to the anomalously large hyperfine coupling between the nuclear magnetic moment and effective magnetic field (H_{eff}) at the Ho nucleus, leading to the ambiguities in the exact estimation of the magnetic heat capacity (C_{m}). The magnetic heat capacity C_{m} is extracted by subtracting the phonon contributions (C_{L}), nuclear contributions (C_{N}) and magnetic Schottky anomaly (C_{sch}) in case of field data from the total heat capacity (shown in figure 5(b)) [29, 30]. The lattice/phononic contribution to heat capacity was estimated by fitting the high-temperature data by using both Einstein and Debye models (and Schottky term in field data) [19]. The value of Debye temperature (Θ_{D}) and Einstein temperature (Θ_{E}) were obtained as 122 K and 305 K, respectively. For $Ho_2Ti_2O_7$, the C_{m} was extracted by subtracting the estimated nuclear contribution (C_{N}) for the pyrochlore oxide Ho_2GaSbO_7 (which shows a peak at $T = 0.3$ K) [3]. Blöte *et al* estimated that the C_{N} arises due to the splitting of eight nuclear levels of holmium (nuclear isospin $I = 7/2$) with the theoretical maximum of $C_{\text{N}} \sim 0.9R$ at $T = 0.3$ K [31]. The obtained value of C_{m} for $Ho_2Ti_2O_7$ using this methodology reveals the same characteristic feature of spin ice as observed for $Dy_2Ti_2O_7$ [32]. Further, the theoretical studies using Monte-Carlo simulation give magnetic entropy values within $\sim$2% of $R[\ln 2 - (1/2)\ln 3/2]$, which agrees well with the ambit of spin ice materials [33]. Such a small variance from the Pauling entropy value could be reasonably accounted for any slight deviations in the hyperfine parameters of $4f$ electrons of rare-earth ions (depending upon ionic surrounding, electric field gradient, etc). Ramon *et al* extracted the nuclear contribution in $Ho_2Zr_2O_7$ by subtracting the nuclear contribution for Ho metal [34]. However, as the low temperature residual magnetic entropy is one of the important quantities to identify the formation of spin ice state, it is necessary to carefully deal with the fitting models to extract the magnetic contribution. Therefore, we have not restricted ourselves to the approaches used by Bramwell *et al*, and Ramon *et al* only for our disordered pyrochlore oxide $Ho_2Zr_2O_7$ because of its modified crystal field spacing associated with the change in lattice and electronic structure. It was found that the hyperfine interactions of Ho spin lead to a nuclear anomaly at $\sim 0.3 \pm 0.02$ K [6, 35, 36]. In contrast, the peak position in $Ho_2Zr_2O_7$ is slightly shifted to a higher temperature of 0.5 K. The subtraction of nuclear part in $Ho_2Zr_2O_7$ is also an approximation as it overshadows the magnetic contribution below $T = 1.5$ K. We have discussed three possible methods to extract the C_{m} for $Ho_2Zr_2O_7$ by subtracting the C_{N} (shown in figure 5(c)) to illustrate the generic effect of structural symmetry and electronic distribution on the heat capacity.

First, the C_{m} was obtained by subtracting the nuclear hyperfine contribution C_{N1} used in the previous reports in case of isostructural Ho_2GaSbO_7 and $Ho_2Ti_2O_7$ [3, 31]. The obtained C_{m} gives a dynamic ground state crossing the entropy limit of $R\ln 2$, expected for the maximum possible states. However, it is hard to rely on this estimation method due to the difference in structural symmetry and effective magnetic moment of $Ho_2Zr_2O_7$ and Ho_2GaSbO_7. Additionally, the observed heat capacity in the systems viz Ho metal, $Ho_2Ti_2O_7$, Ho_2GaSbO_7 pyrochlore, $HoCrO_3$ distorted perovskite, shows a variation of $\sim$2–6% in the peak position and magnitude of C_{N} [6, 35–37]. Therefore in the second case, we have fixed the peak position to 0.3 K and tried to fit the C_{N} of $Ho_2Zr_2O_7$ ($I = 7/2$) using the equation [38]

$$C_{\text{N}} = \frac{R\sum_{i=-I}^{I}\sum_{j=-I}^{I}(W_i^2 - W_iW_j)\mathrm{e}^{\frac{-W_i-W_j}{kT}}}{(kT)^2\sum_{i=-I}^{I}\sum_{j=-I}^{I}\mathrm{e}^{\frac{-W_i-W_j}{kT}}} \qquad (1)$$

where R is universal gas constant, $W_i/k = a'i + P[i^2 - I(I+1)/3]$, $a' = 0.299 \pm 0.002$ K is measure of the strength of hyperfine interactions and P represents the quadrupole coupling constant which is negligible in case of holmium. The obtained nuclear hyperfine contribution C_{N2} is shown in figure 5(c). Remarkably, the additional constraints due to the substitution of Zr for Ti could account for the change in hyperfine interactions, the resulting peak position and magnitude of C_{N}. In the third case, we have used the hyperfine interaction model (C_{N3}) to fit the raw data without approximating the magnitude or the nuclear peak position. We estimated that the total uncertainty in the extracted data is more than $\sim$10% due to the uncertainty in the subtraction of nuclear spin contribution. Figures 5(d) and (e) shows the extracted C_{m} data at $H = 0$ and 5 kOe where C_{m1}, C_{m2}, C_{m3} are the extracted magnetic contributions according to the three different fitting approaches

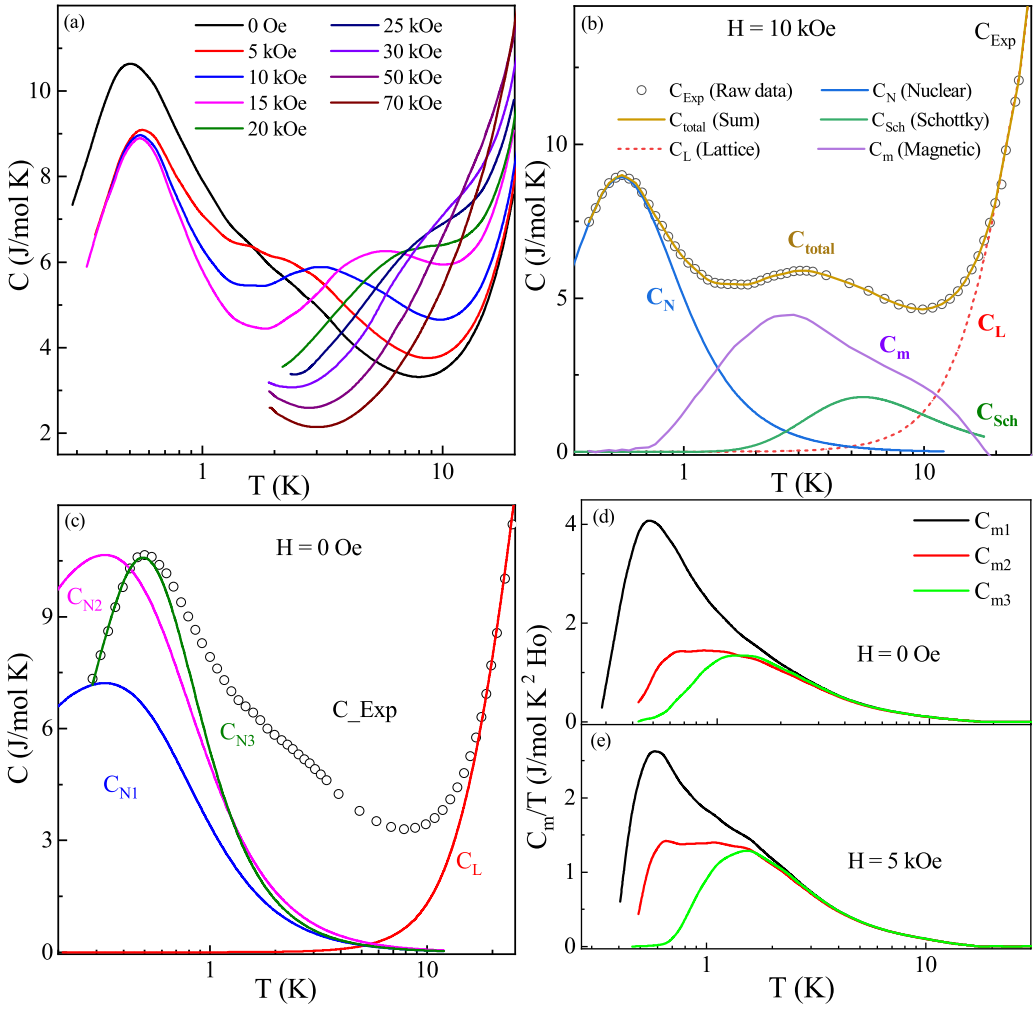

Figure 5. (a) Temperature dependence of heat capacity data at various magnetic fields between 0–70 kOe. (b) Heat capacity data analysis of $Ho_2Zr_2O_7$ at $H = 10$ kOe using various fitting models. (c) Nuclear heat capacity data analysis of $Ho_2Zr_2O_7$ at $H =$ Oe using three different approaches as explained in the main text. (d) and (e) Shows the temperature dependence of C_m/T at $H = 0$, 5 kOe. The components C_{m1}, C_{m2} and C_{m3} represent the magnetic heat capacity extracted using the different approaches discussed in the main text.

and correspondingly the ΔS_{m1}, ΔS_{m2}, ΔS_{m3} are the magnetic entropy changes (shown in figure 6(a)).

The recovered entropy of (ΔS_m) was calculated by integrating the C_m/T from $T = 0.3$–12 K. We have plotted ΔS_m of $Ho_2Zr_2O_7$ obtained at $H = 0$ from the above mentioned three methods along with the ΔS_m for spin ice $Ho_2Ti_2O_7$ taken from reference [3] in figure 6(a). In the absence of a magnetic field, the ΔS_m (third case) is comparatively lower than for the disordered state value of $R \ln 2$ corresponding to the maximum possible 2^N states available to N spins, which indicates that the residual entropy is small compared to the spin ice value as T goes to zero. The $Ho_2Ti_2O_7$ is reported to show Pauling's value of water ice $(R/2)\ln(3/2)$ at zero magnetic field [3]. The integrated entropy for $Ho_2Zr_2O_7$ is larger than that for $Ho_2Ti_2O_7$, indicating a significant decrease in the zero-point entropy. It is to mention that the heat capacity fitting performed for an even larger temperature range up to 35 K did not show evidence of missing entropy. The increase in entropy is understood from the chemical alteration of the pyrochlore structure with Zr substitution. The partial replacement of Dy or Ho site in $(Dy/Ho)_{2-x}Y_xTi_2O_7$ by non-magnetic Y, Lu strongly affect the spin ice state, however, the lattice structure remains intact [6, 39]. Figure 6(b) shows the recovered value of ΔS_m at various magnetic fields taken at $T = 12$ K. Application of a magnetic field to the degenerate ground state restored some of the missing entropy, presumably due to the lifted degeneracy of the ground state as the applied field breaks the system's symmetry. An additional peak appears at $T > 3$ K on switching the magnetic field and shift to higher temperatures with an increase in the magnetic field. This also shows a continuous decrease in magnetic entropy, leading to a non-magnetic ground state at 70 kOe. We have also fitted the heat capacity data of $Ho_2Ti_2O_7$ taken from reference [3] using the same hyperfine model (inset of figure 6(b)). Amazingly, the extracted magnetic entropy is significantly lower ($\sim$12%) than the expected value for the spin ice systems. Thus the approach of using the nuclear contribution of Ho_2GaSbO_7 by Blöte *et al* is not a good choice for the estimation of magnetic heat capacity of $Ho_2Ti_2O_7$ compound. Similarly, the use of estimated nuclear heat capacity of $Dy_3Ga_5O_{12}$ garnet to $Dy_2Ti_2O_7$ is suggested to be

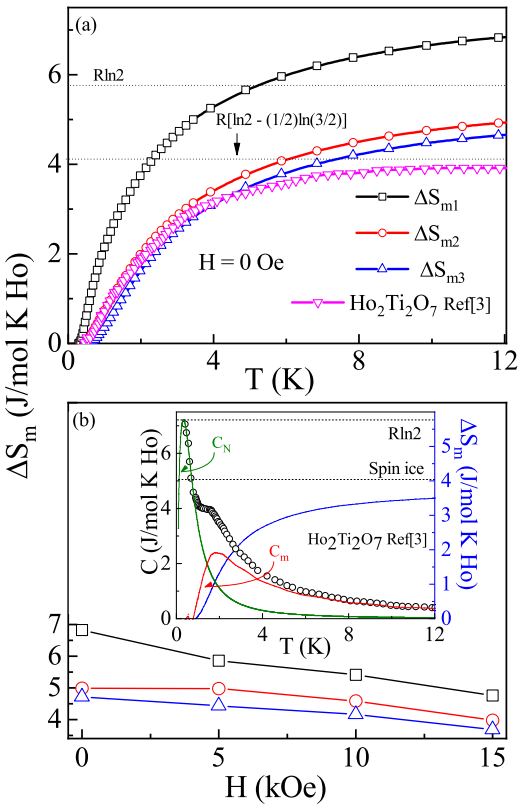

Figure 6. (a) Temperature dependence of extracted magnetic entropy (ΔS_{m1}, ΔS_{m2} and ΔS_{m3} extracted using three methodologies) of $Ho_2Zr_2O_7$ at $H = 0$ Oe and zero field data of spin ice $Ho_2Ti_2O_7$ taken from the reference [3]. (b) Variation in the magnetic entropy of $Ho_2Zr_2O_7$ in reference [3] as a function of applied field. Inset shows the heat capacity data (symbol) of $Ho_2Ti_2O_7$ fitted (green) with hyperfine model (equation (1)), extracted magnetic heat capacity (red) and the magnetic entropy (blue).

incorrect due to the difference between the magnitude of moments ($Dy_3Ga_5O_{12}$: $\mu_{eff} \sim 4.5\ \mu_B$ and $Dy_2Ti_2O_7$: $\mu_{eff} \sim 9.8\ \mu_B$) [32].

In conclusion, $Ho_2Zr_2O_7$ with its disordered pyrochlore structure shows the presence of spin freezing at $T \sim 10$ K on the application of the magnetic field. Unlike the spin ice systems, the heat capacity and susceptibility indicate large spin dynamics at the lowest measuring temperature and the absence of Pauling residual entropy. These studies show that the low-temperature magnetic state of pyrochlores systems can be significantly altered by frustration and structural disorder. We have further analyzed the low-temperature heat capacity and discussed the error arising from the estimation of nuclear contribution in holmium based system. We observed that the use of the hyperfine model (equation (1)) for the estimation of nuclear heat capacity leads to the significant correction in the residual spin ice entropy of the $Ho_2Ti_2O_7$. The disordered pyrochlore zirconates provide an excellent family of materials for further investigation, for the role of induced disorder on the spin dynamics and the creation/propagation of monopole–antimonopole excitations in the frustrated systems. The low-temperature neutron scattering technique would be important for the identification of true magnetic ground state in $Ho_2Zr_2O_7$.

Acknowledgment

We thank AMRC, Indian Institute of Technology Mandi for the experimental facility. Sheetal acknowledged IIT Mandi and MHRD India for the HTRA fellowship. We acknowledge financial support by BMBF via the Project Spin-Fun (13XP5088) and by Deutsche Forschungsgemeinschaft (DFG) under Germany's Excellence Strategy EXC2181/1-390900948 (the Heidelberg STRUCTURES Excellence Cluster) and through Project KL 1824/13-1.

Data availability statement

All data that support the findings of this study are included within the article (and any supplementary files).

ORCID iDs

Sheetal https://orcid.org/0000-0002-4766-0108
A Elghandour https://orcid.org/0000-0001-8289-2644
R Klingeler https://orcid.org/0000-0002-8816-9614
C S Yadav https://orcid.org/0000-0002-0664-5489

References

[1] Matsuhira K, Hinatsu Y and Sakakibara T 2001 Novel dynamical magnetic properties in the spin ice compound $Dy_2Ti_2O_7$ *J. Phys.: Condens. Matter* **13** L737
[2] Ramirez A P, Hayashi A, Cava R J, Siddharthan R and Shastry B 1999 Zero-point entropy in 'spin ice' *Nature* **399** 333
[3] Bramwell S *et al* 2001 Spin correlations in $Ho_2Ti_2O_7$: a dipolar spin ice system *Phys. Rev. Lett.* **87** 047205
[4] Snyder J, Slusky J, Cava R J and Schiffer P 2001 How 'spin ice' freezes *Nature* **413** 48
[5] Snyder J, Ueland B, Slusky J, Karunadasa H, Cava R J and Schiffer P 2004 Low-temperature spin freezing in the $Dy_2Ti_2O_7$ spin ice *Phys. Rev.* B **69** 064414
[6] Lau G, Freitas R, Ueland B, Muegge B, Duncan E, Schiffer P and Cava R 2006 Zero-point entropy in stuffed spin-ice *Nat. Phys.* **2** 249
[7] Ehlers G, Cornelius A, Orendac M, Kajnakova M, Fennell T, Bramwell S and Gardner J 2002 Dynamical crossover in 'hot' spin ice *J. Phys.: Condens. Matter* **15** L9
[8] Kimura K, Nakatsuji S, Wen J, Broholm C, Stone M, Nishibori E and Sawa H 2013 Quantum fluctuations in spin-ice-like $Pr_2Zr_2O_7$ *Nat. Commun.* **4** 1934
[9] Wen J-J *et al* 2017 Disordered route to the coulomb quantum spin liquid: random transverse fields on spin ice in $Pr_2Zr_2O_7$ *Phys. Rev. Lett.* **118** 107206
[10] Petit S *et al* 2016 Observation of magnetic fragmentation in spin ice *Nat. Phys.* **12** 746
[11] Ramon J, Wang C, Ishida L, Bernardo P, Leite M, Vichi F, Gardner J and Freitas R 2019 Absence of spin-ice state in the disordered fluorite $Dy_2Zr_2O_7$ *Phys. Rev.* B **99** 214442
[12] Sibille R *et al* 2017 Coulomb spin liquid in anion-disordered pyrochlore $Tb_2Hf_2O_7$ *Nat. Commun.* **8** 892
[13] Anand V, Islam A, Samartzis A, Xu J, Casati N and Lake B 2018 Optimization of single crystal growth of candidate quantum spin-ice $Pr_2Hf_2O_7$ by optical floating-zone method *J. Cryst. Growth* **498** 124
[14] Anand V, Tennant D and Lake B 2015 Investigations of the effect of nonmagnetic Ca substitution for magnetic Dy on spin-freezing in $Dy_2Ti_2O_7$ *J. Phys.: Condens. Matter* **27** 436001

[15] Mouta R, Silva R and Paschoal C 2013 Tolerance factor for pyrochlores and related structures *Acta Crystallogr.* B **69** 439

[16] Sheetal and Yadav C S 2021 Evolution of spin freezing transition and structural, magnetic phase diagram of $Dy_{2-x}La_xZr_2O_7$ ($0 \leqslant x \leqslant 2.0$) *Sci. Rep.* **11** 19832

[17] Anand V *et al* 2016 Physical properties of the candidate quantum spin-ice system $Pr_2Hf_2O_7$ *Phys. Rev.* B **94** 144415

[18] Anand V, Bera A, Xu J, Herrmannsdörfer T, Ritter C and Lake B 2015 Observation of long-range magnetic ordering in pyrohafnate $Nd_2Hf_2O_7$: a neutron diffraction study *Phys. Rev.* B **92** 184418

[19] Sheetal , Ali A, Rajput S, Singh Y, Maitra T and Yadav C S 2020 Emergence of weak pyrochlore phase and signature of field induced spin ice ground state in $Dy_{2-x}La_xZr_2O_7$; $x = 0, 0.15, 0.3$ *J. Phys.: Condens. Matter* **32** 365804

[20] Xu J, Islam A, Glavatskyy I, Reehuis M, Hoffmann J-U and Lake B 2018 Field-induced quantum spin-1/2 chains and disorder in $Nd_2Zr_2O_7$ *Phys. Rev.* B **98** 060408

[21] Zhang F, Lang M, Becker U, Ewing R and Lian J 2008 High pressure phase transitions and compressibilities of $Er_2Zr_2O_7$ and $Ho_2Zr_2O_7$ *Appl. Phys. Lett.* **92** 011909

[22] Ehlers G, Cornelius A, Fennell T, Koza M, Bramwell S and Gardner J 2004 Evidence for two distinct spin relaxation mechanisms in 'hot' spin ice $Ho_2Ti_2O_7$ *J. Phys.: Condens. Matter* **16** S635

[23] Rodríguez-Carvajal J 1990 FULLPROF: a program for Rietveld refinement and pattern matching analysis *Satellite Meeting on Powder Diffraction of the XV Congress of the IUCr* vol 127 (Toulouse, France)

[24] Mandal B, Garg N, Sharma S M and Tyagi A 2006 Preparation, xrd and Raman spectroscopic studies on new compounds $RE_2Hf_2O_7$ (RE = Dy, Ho, Er, Tm, Lu, Y): pyrochlores or defect-fluorite? *J. Solid State Chem.* **179** 1990

[25] Harris M J, Bramwell S, McMorrow D, Zeiske T and Godfrey K 1997 Geometrical frustration in the ferromagnetic pyrochlore $Ho_2Ti_2O_7$ *Phys. Rev. Lett.* **79** 2554

[26] den Hertog B C and Gingras M J 2000 Dipolar interactions and origin of spin ice in Ising pyrochlore magnets *Phys. Rev. Lett.* **84** 3430

[27] Shukla M, Upadhyay R, Tolkiehn M and Upadhyay C 2020 Robust spin-ice freezing in magnetically frustrated $Ho_2Ge_xTi_{2-x}O_7$ pyrochlore *J. Phys.: Condens. Matter* **32** 465804

[28] Binder K and Young A P 1986 Spin glasses: experimental facts, theoretical concepts, and open questions *Rev. Mod. Phys.* **58** 801

[29] Lal S, Mukherjee K and Yadav C 2018 Effect of crystalline electric field on heat capacity of $LnBaCuFeO_5$ (Ln = Gd, Ho, Yb) *Solid State Commun.* **270** 130

[30] Ku S *et al* 2018 Low temperature magnetic properties of $Nd_2Ru_2O_7$ *J. Phys.: Condens. Matter* **30** 155601

[31] Blöte H, Wielinga R and Huiskamp W 1969 Heat-capacity measurements on rare-earth double oxides $R_2M_2O_7$ *Physica* **43** 549

[32] Henelius P, Lin T, Enjalran M, Hao Z, Rau J, Altosaar J, Flicker F, Yavorskii T and Gingras M 2016 Refrustration and competing orders in the prototypical $Dy_2Ti_2O_7$ spin ice material *Phys. Rev.* B **93** 024402

[33] Den Hertog B, Gingras M J, Bramwell S T and Harris M J 1999 Comment on Ising pyrochlore magnets: low temperature properties, 'ice rules', and beyond by R Siddharthan *et al* *Phys. Rev. Lett.* **83** 1854

[34] Ramón J G A 2020 Geometrically frustrated magnetism in the pyrochlore $Er_2Ti_{2-x}Sn_xO_7$ and in the disordered fluorites $R_2Zr_2O_7$ (R = Dy, Ho, Tb) *PhD Thesis* Universidade de São Paulo

[35] Kumar C, Xiao Y, Nair H, Voigt J, Schmitz B, Chatterji T, Jalarvo N and Brückel T 2016 Hyperfine and crystal field interactions in multiferroic $HoCrO_3$ *J. Phys.: Condens. Matter* **28** 476001

[36] Nagata S, Sasaki H, Suzuki K, Kiuchi J and Wada N 2001 Specific heat anomaly of the holmium garnet $Ho_3Al_5O_{12}$ at low temperature *J. Phys. Chem. Solids* **62** 1123

[37] Krusius M, Anderson A and Holmström B 1969 Calorimetric investigation of hyperfine interactions in metallic Ho and Tb *Phys. Rev.* **177** 910

[38] Lounasmaa O 1962 Specific heat of holmium metal between 0.38 and 4.2 K *Phys. Rev.* **128** 1136

[39] Snyder J, Ueland B, Mizel A, Slusky J, Karunadasa H, Cava R and Schiffer P 2004 Quantum and thermal spin relaxation in the diluted spin ice $Dy_{2-x}M_xTi_2O_7$ (M = Lu, Y) *Phys. Rev.* B **70** 184431